https://doi.org/10.35877/jetech4411

OPEN ACCESS

ISSN : 2776-7914 (Print) / 2807-3045 (Online)

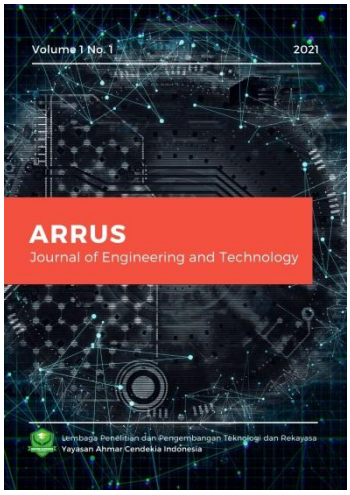

RESEARCH ARTICLE

Reservoir Characterization Using Integrated Seismic Inversion and Multiattribute Analysis Based on Probabilistic Neural Network (PNN)

Amelia Kartika[1*], Handoyo Handoyo[1], Asido Saputra Sigalingging[1], Farizki Budi Pangestu[2], Mochammad Wafa Husain[3]

[1]Department of Geophysical Engineering, Institut Teknologi Sumatera, Lampung, Indonesia
[2]Department of Geophysical Engineering, UPN "Veteran" Yogyakarta, Yogyakarta, Indonesia
[3]Department of Geophysical Engineering, Universitas Brawijaya, Malang, Indonesia

*Correponding Author: Amelia Kartika, Department of Geophysical Engineering, Institut Teknologi Sumatera, Lampung, Indonesia.

Email: ameliakartika405@gmail.com

Abstract: The 3D seismic acquisition in the Volve Field, located in the North Sea Basin, Norway, was conducted to explore the hydrocarbon potential of the Hugin Formation, which was deposited during the Mesozoic era. The analyzed dataset consists of 3D Post Stack Time Migration (PSTM) and well log data (sonic, density, and porosity) to support the interpretation process. This study aims to characterize the reservoir zone through the integration of Acoustic Impedance (AI) seismic inversion and multiattribute analysis using the Probabilistic Neural Network (PNN) method. Seismic inversion was employed to generate AI sections that represent variations in the physical properties of rocks, while the PNN based multiattribute analysis was applied to nonlinearly predict the porosity log distribution from seismic data. The results indicate that the sandstone reservoir within the Hugin Formation has AI values ranging from 7,000 to 9,000 (g/cc·m/s) and porosity values from 0.15 to 0.30 (v/v). The integration of these two methods has proven effective in enhancing the resolution of reservoir characterization and delineating hydrocarbon prospect zones in the Volve Field.

Keywords: Hugin Formation, Acoustic Impedance Inversion, Reservoir Characterization, Probabilistic Neural Network, Seismic Reflection.

1. Introduction

Reservoir characterization is an important component in hydrocarbon exploration and development, because the ability to identify petrophysical distribution and describe lithological and fluid variations greatly influences field development decisions. However, conventional seismic reflection methods often face limitations when evaluating thin layers or heterogeneous intervals, resulting in insufficient resolution for accurate lithological and fluid mapping (Leite & Vidal, 2011). To overcome these limitations, the integration of AI based inversion with multiattribute analysis using PNN offers a more sophisticated and adaptive approach to data. Seismic inversion generates quantitative subsurface models through sections generated by AI, while PNN based multiattribute analysis improves petrophysical property estimates by capturing nonlinear relationships between seismic attributes (Ardinda & Riyanto, 2020). Compared to traditional linear regression or deterministic methods, the PNN framework provides superior performance in managing geological complexity and reducing interpretation uncertainty. The combined application of AI inversion and PNN

https://doi.org/10.35877/jetech4411

ISSN : 2776-7914 (Print) / 2807-3045 (Online)

based analysis has proven effective in improving spatial resolution and sharpening hydrocarbon prospect mapping, especially in complex geological reservoirs (Rizqi & Firdaus, 2021).

The Volve field, located in the North Sea within the Hugin Formation, is an ideal case study for applying seismic and well integration with PNN due to its stratigraphic complexity and highly varied lithology of productive sandstone (Sanderson, 1991). Previous studies in the Volve Field have shown that deterministic and stochastic seismic inversion methods can produce elastic parameters that are sensitive to lithology and fluid content, such as the Vp/Vs ratio and Poisson's ratio. These parameters are widely used as indicators of sandstone lithology and hydrocarbon bearing zones (Pelemo-Daniels & Stewart, 2024).

The integration of AI inversion with PNN based multiattribute analysis is expected to improve spatial resolution and increase the accuracy of reservoir parameter estimates, thereby providing clearer mapping of prospective hydrocarbon zones in the Hugin Formation, particularly in the Volve Field. The data used in this study consists of 3D PSTM seismic data and well logs, including sonic, density, and porosity logs. The Hugin Formation was selected because it represents one of the main stratigraphic intervals dominated by sandstone lithology with significant hydrocarbon reservoir potential. The application of these two methods is expected to produce more accurate AI distribution maps and porosity predictions to support the mapping of hydrocarbon bearing zones in the Volve Field.

2. Geology of the North Sea

The geological framework of the North Sea provides the foundation for understanding its hydrocarbon potential and structural evolution (Person & Peter, 1998). A detailed overview of the regional geology, including the distribution of major grabens and sedimentary sequences, is illustrated in Figure 1, which highlights the key structural and stratigraphic elements that control reservoir development across the basin.

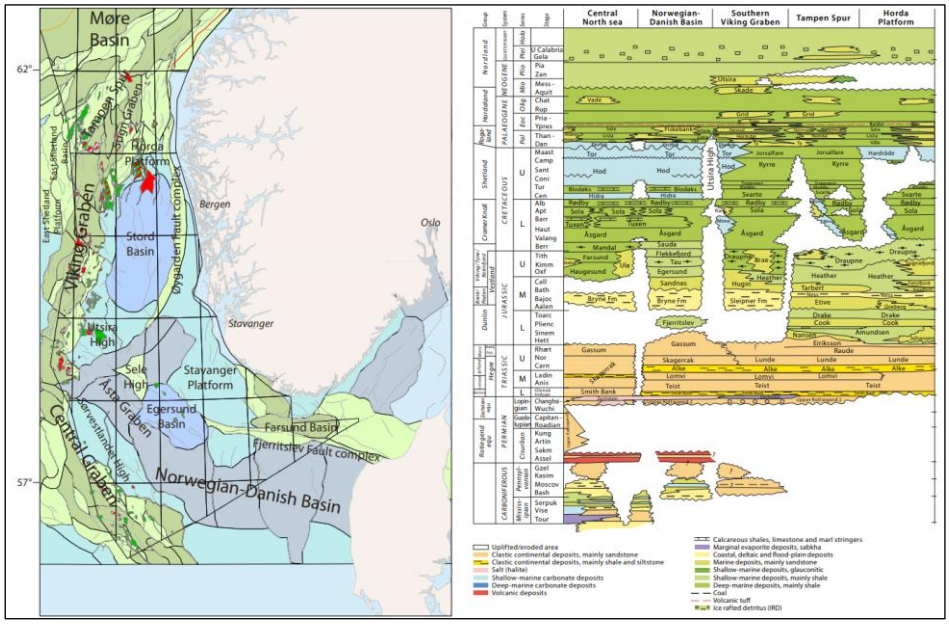

Figure 1 Geology of the North Sea (Person & Peter, 1998)

Within this geological framework, the Hugin Formation is located in the southern Viking Graben, overlying the deltaic coal bearing Sleipner Formation and overlain by the shales of the Viking Group. The formation, up to 174 m was deposited in a nearshore to shallow marine environment with fluvio deltaic influence. Its thickness decreases eastward and northward, partly controlled by salt tectonics. At the Sleipner West Field, the formation occurs at approximately 3,400 m depth, with porosity ranging from 16 to 20 (%) and

https://doi.org/10.35877/jetech4411

ISSN : 2776-7914 (Print) / 2807-3045 (Online)

permeability between 0.1 to 400 (mD), signifying excellent reservoir quality, as illustrated in Figure 2, which shows the geological framework of the Hugin Formation.

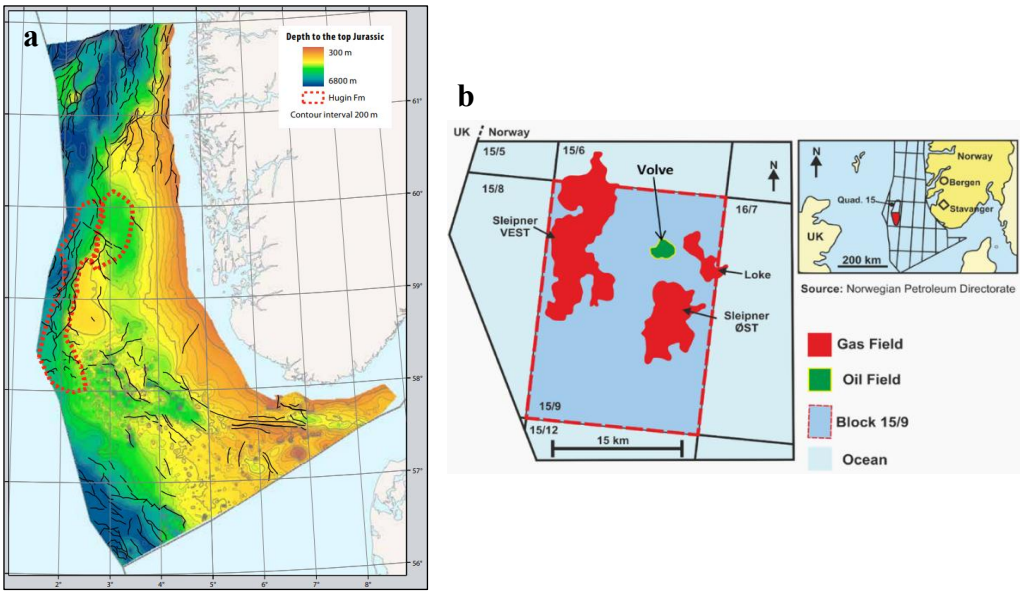

Figure 2 (a) Geology of the Hugin Formation (b) location map of Volve Field (Person & Peter, 1998)

The study area is located in Block F15/9 of the Norwegian sector of the North Sea Basin, adjacent to the Sleipner Field in the southern part of the Viking Graben. This area lies within a structurally complex fault zone, characterized by a normal fault system that influences sedimentation patterns and hydrocarbon migration pathways. Its proximity to the Sleipner Field provides a well documented geological framework, where the Hugin Formation serves as the main reservoir unit formed in a coastal deltaic to shallow marine environment during the Middle Jurassic period. The structural configuration and stratigraphic continuity in Block F15/9 make it an ideal location for applying integrated seismic inversion and PNN based multiattribute analysis to investigate reservoir heterogeneity and identify zones with hydrocarbon potential.

3. Research Method and Materials

3.1. Acoustic Impedance (AI)

AI is a physical property that describes the ability of a medium to transmit seismic waves (Zwaan et al., 2022). It is mathematically defined as the product of rock density (ρ) and seismic wave velocity (Vp), as expressed in equation (1):

$$AI = \rho \cdot Vp \tag{1}$$

The unit of AI (g/cc·m/s), and velovity (m/s). Physically, AI increases with both the density and velocity of the rock, indicating that harder and more compact formations exhibit higher impedance values. Variations in AI between layers are fundamental in seismic reflection analysis, as they determine the reflection coefficient that governs the strength and polarity of reflected seismic signals (Chasandra et al., 2018).

3.2. Multiattribute Probabilistic Neural Network (PNN)

PNN introduced by Specht (1990), is employed to correlate seismic attributes with well log data through a Gaussian probability based approach (Specht, 1990). PNN method is a statistical approach used to model nonlinear relationships between seismic attributes and petrophysical parameters, such as porosity or AI. PNN operates by estimating the degree of

https://doi.org/10.35877/jetech4411

ISSN : 2776-7914 (Print) / 2807-3045 (Online)

similarity between input data and training samples through a Gaussian probability function, as expressed in equation (2):

$$\rho_{nk}(\sigma) = exp\left[-\frac{1}{2}\sum_{j=1}^{J}\left(\frac{a_{Jk-}a_{Jn}}{2\sigma_J}\right)^2\right] \quad (2)$$

This equation indicates that the smaller the difference between the seismic attribute values (a_{jk} and a_{jn}), the higher the probability value $\rho_{nk}(\sigma)$, representing a greater similarity between data points. The parameter σ serves as a smoothing factor, controlling the width of the Gaussian distribution larger values produce broader distributions, while smaller values yield sharper ones.

The predicted log value L_k is then calculated as a weighted average of the actual log value L_n using the probability weights $\rho_{nk}(\sigma)$, as expressed in equation (3):

$$\hat{L}_k = \frac{\sum_{n=1}^{N}\rho_{nk}(\sigma)L_n}{\sum_{n=1}^{N}\rho_{nk}(\sigma)} \quad (3)$$

Through this process, PNN minimizes the error between actual and predicted log values, resulting in more accurate estimations of reservoir parameters. This method has proven effective in characterizing lithological variations and mapping porosity distribution based on seismic response data.

The objective function is formulated to minimize the discrepancy between the measured k values and the log values predicted by the model, as expressed in equation (4):

$$[E(\sigma)] = \sum_{k=1}^{k}[L_k - L_k(\sigma)]^2 \quad (4)$$

Represents the total squared error across all training samples. Once the model is "trained" to obtain an optimal value of σ, this function can be used to predict the log L_k for each well and subsequently propagate the predicted property throughout the seismic volume (Specht, 1990).

The methodological approach in this study follows a structured sequence that integrates seismic and well data to support a consistent and quantitative reservoir analysis. The following subsections describe each stage applied in the workflow:

3.3. Seismic Data

The seismic data used in this study were acquired from the North Sea region and consist of 3D PSTM. The dataset comprises 401 inlines (9,961 to 10,361) and 720 xlines (1,961 to 2,680), providing sufficient spatial coverage for detailed structural and stratigraphic interpretation. Figure 3 presents the frequency range in seismic data, dominant frequency of the seismic volume is approximately 24 Hz, which offers a good balance between vertical resolution and signal to noise ratio. The frequency components used in the analysis range from F1 = 0 Hz, F2 = 14 Hz, F3 = 42 Hz, to F4 = 56 Hz, ensuring that both low and high frequency information is preserved during inversion. Figure 4 presents the seismic section across the well, clearly depicting the stratigraphic continuity, reflector geometry, and the overall quality of the seismic data used in this study.

https://doi.org/10.35877/jetech4411

OPEN ACCESS

ISSN : 2776-7914 (Print) / 2807-3045 (Online)

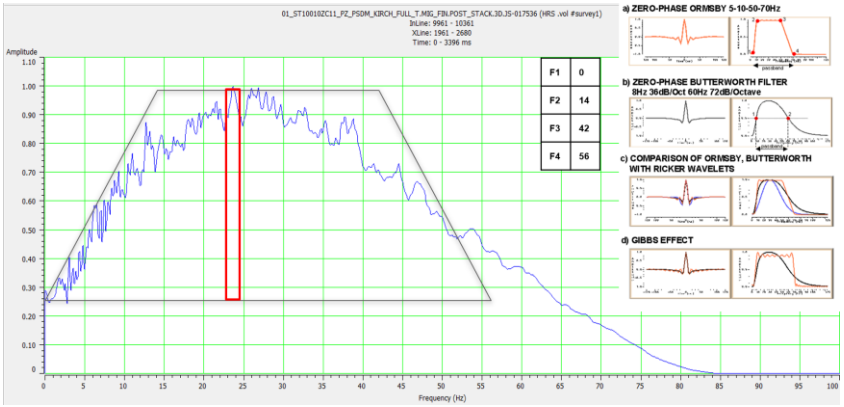

Figure 3 The frequency range in seismic data

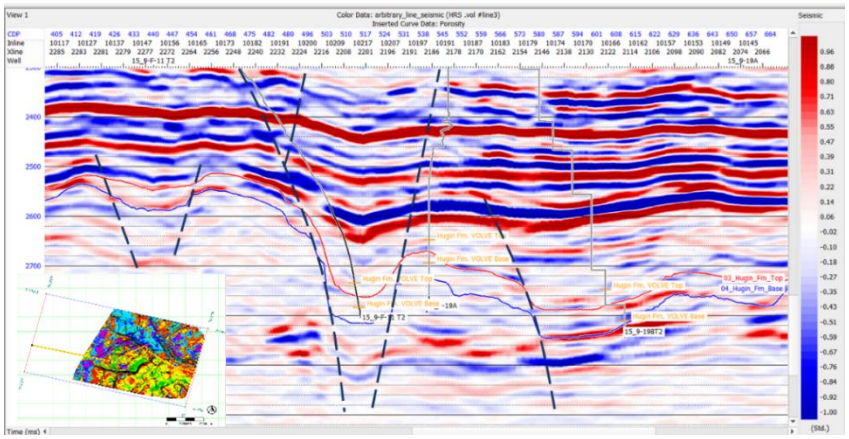

Figure 4 Seismic section across the well

3.4. Well Data

This study uses three wells 15/9-19A, 15/9-19BT2, and 15/9F-11T2 located in Block F15/9 of the North Sea near the Sleipner area. Each well contains a comprehensive log, but gamma ray, P-wave velocity, density, and porosity logs were selected as key inputs for seismic inversion and PNN analysis. The gamma ray log delineates lithological boundaries, while sonic and density logs provide AI inputs. The porosity log serves as the main petrophysical parameter for reservoir characterization. Figure 5 displays the well correlation, confirming uniform stratigraphic layering across the study area. Show the wells penetrate the Hugin Formation at depths ranging up to 3,700 m, intersecting interbedded sandstone and shale sequences deposited in a shallow marine deltaic setting.

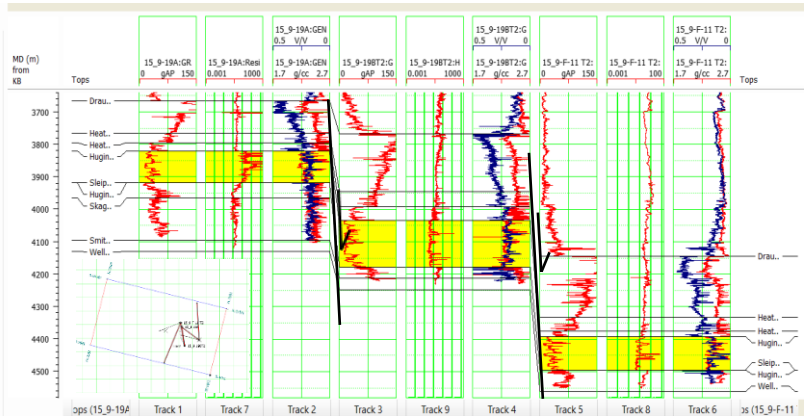

Figure 5 Correlation of each well with the main stratigraphic markers

https://doi.org/10.35877/jetech4411

ISSN : 2776-7914 (Print) / 2807-3045 (Online)

3.5. *Wavelet Extraction and Well Seismic Tie*

The statistical wavelet extraction was carried out within the Hugin Formation interval to capture the dominant frequency response of the seismic data (24 Hz) and ensure that the extracted wavelet accurately represents the local spectral and phase characteristics of the subsurface. This approach minimizes external bias from assumed source signatures and tailors the wavelet specifically to the geological and acquisition conditions of the study area.

The extracted wavelet was subsequently applied in the Well Seismic Tie (WST) process, which aligns the measured depth domain from well logs with the Two Way Time (TWT) domain of seismic reflection data. This calibration ensures that key geological markers such as the top and base Hugin horizons correspond precisely to their seismic reflectors. The WST achieved a high correlation coefficient of 0.7 to 0.9 between synthetic and observed seismic traces, indicating excellent phase and polarity consistency, as well as an accurate amplitude match. This well calibrated wavelet provides the foundation for the AI inversion by ensuring that the seismic reflectivity is physically linked to true rock property variations. The outcomes of this calibration, illustrated in Figure 6 and summarized in Table 1, confirm that the extracted wavelet is well suited for quantitative interpretation and reservoir characterization.

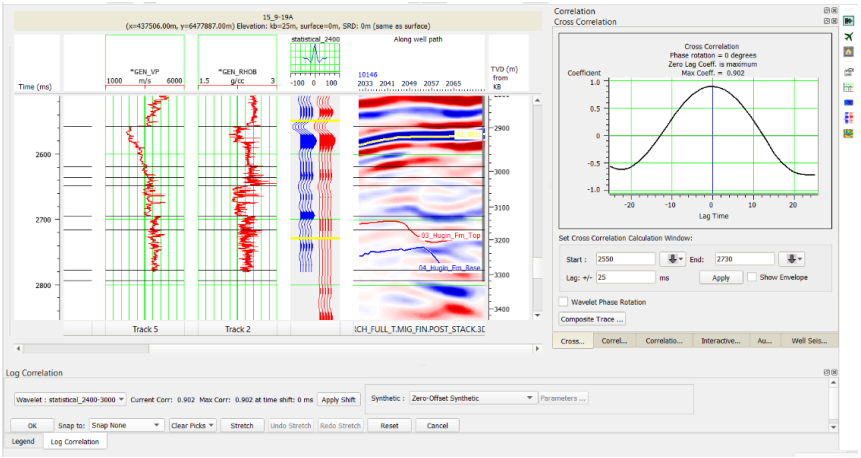

Figure 6 WST at well 15/9-19A

Table 1 WST values for each well

Well	Wavelet	Wavelength	Correlation
15/9-19A			0.902
15/9-19BT2	Statistical	100	0.909
15/9-F T2			0.781

3.6. *Horizon Interpretation*

Horizon picking was performed by identifying and tracking seismic reflectors that exhibit continuous layering on the seismic section. This process aims to determine stratigraphic boundaries and geological structures relevant to the target zone. Geological context, depositional environment, and the direction of reservoir facies distribution serve as important references to ensure the accuracy of horizon interpretation.

3.7. *Sensitivity Analysis*

The crossplot between AI and porosity is used to identify reservoir and non-reservoir zones based on the distribution patterns observed in Figure 7 and the sensitivity criteria summarized in Table 2. The relationship between these parameters produces a clear separation between porous sandstone and more compact lithologies, enabling reliable determination of lithology and reservoir quality cutoffs. This zonation framework was subsequently applied as a

https://doi.org/10.35877/jetech4411

ISSN : 2776-7914 (Print) / 2807-3045 (Online)

calibration reference for AI inversion and as a key constraint in PNN based porosity modeling, ensuring that all analytical steps remain consistent with the measured physical characteristics of the reservoir. Quantitatively, the reservoir zone is characterized by AI values ranging from 7,000 to 9,000 (g/cc·m/s), density between 2.15 to 2.35 (g/cc), and porosity values from 0.15 to 0.30 (v/v). In contrast, non-reservoir intervals exhibit AI >9,000 g/cc·m/s, density >2.40 g/cc, and porosity <0.12 v/v.

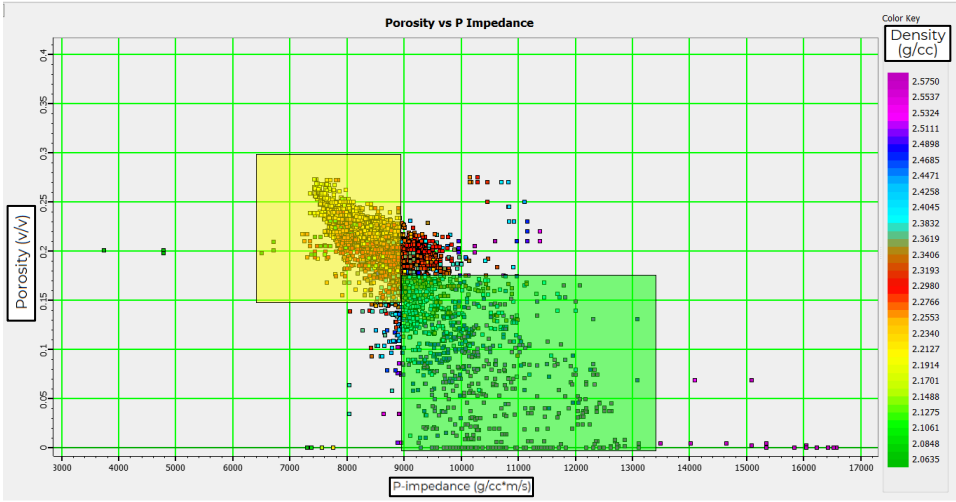

Figure 7 Zonation of p-impedance vs. porosity in density color key

Table 2 Sensitivity analysis of AI and porosity values

Sensitivity Analysis	Reservoir	Non-reservoir
AI (g/cc·m/s)	7,000-9,000	9,000-13,000
Porosity (v/v)	0.15-0.30	0-0.15

3.8. Initial Inversion Model

The initial model was generated using 3D seismic volumes, extracted statistical wavelets, and interpreted structural horizons, with the wells providing essential calibration controls. These horizons guided the extrapolation of well log properties into the seismic volume, allowing the AI distribution to follow the geological framework of the Hugin Formation. The resulting model shows consistent impedance trends that are consistent with the well log response, and provides a strong starting point for the inversion workflow. Figure 8 shows the initial AI model.

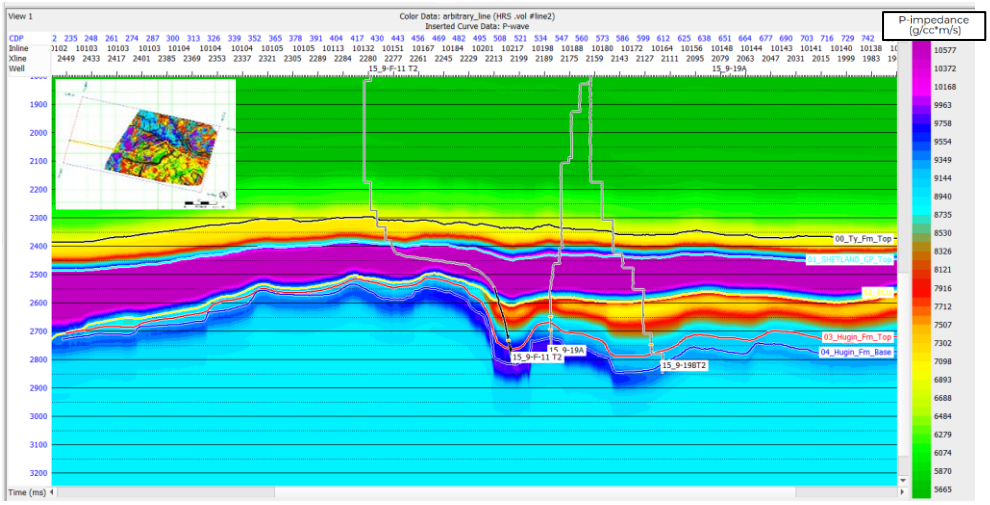

Figure 8 Initial inversion model from the arbitrary line

https://doi.org/10.35877/jetech4411

ISSN : 2776-7914 (Print) / 2807-3045 (Online)

3.9. AI Inversion Parameter Analysis

AI inversion parameter analysis was performed to obtain the optimal parameter combination that produced the highest conformity between synthetic data and actual seismic data. This stage aimed to ensure that the inversion process produced an impedance model that represented the subsurface geological conditions. The evaluation was performed by comparing the error values between the inverted AI log and the well log, as well as by assessing the correlation level between the synthetic trace and the seismic trace. Figure 9 shows the results of the optimal inversion parameter analysis, which is used as a reference for the main inversion process throughout the study area.

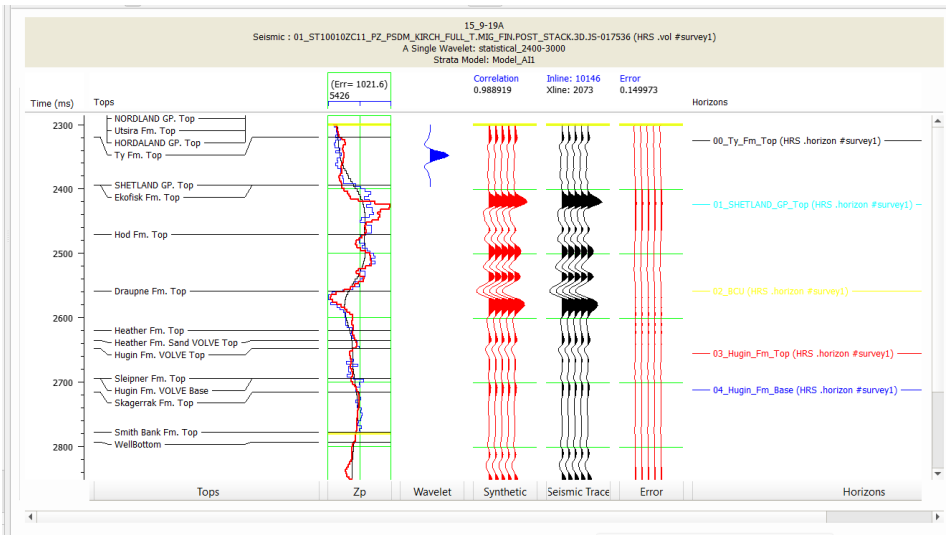

Figure 9 Analysis parameters for well 15/9-19A in model based inversion

3.10. PNN Multiattribute Analysis

In this study, porosity estimation was developed using well log porosity as the target and a set of selected seismic attributes as predictors. The multiattribute workflow was further enhanced using a PNN to capture nonlinear relationships between the seismic data and petrophysical properties. Attribute selection was based on training and validation error performance to identify the most effective attribute combinations for porosity prediction. Figure 10 and Table 3 present the resulting training and validation errors from the multiattribute PNN analysis.

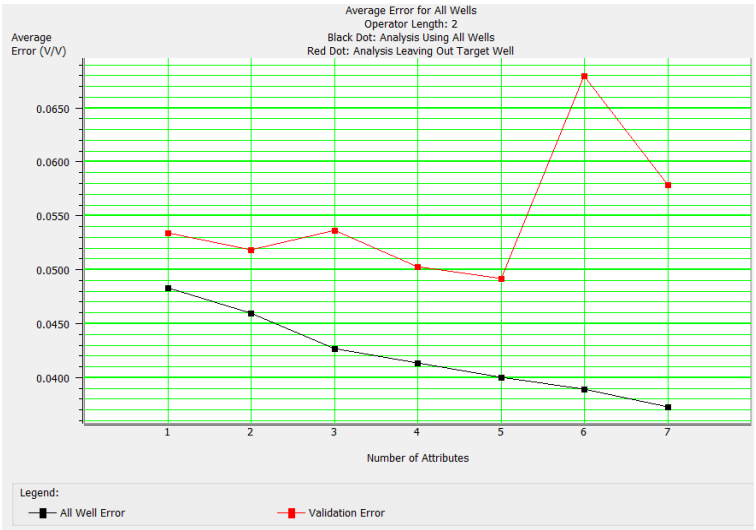

Figure 10 Training and validation error graphs in multiattribute analysis using the five best attribute combinations

https://doi.org/10.35877/jetech4411

ISSN : 2776-7914 (Print) / 2807-3045 (Online)

Table 3 Training and validation errors in multiattribute analysis using the five best attribute combinations

No.	Target	Final Attribute	Training Error	Validation Error
1	Porosity	Integrate	0.048393	0.053485
2		Amplitude Envelope	0.045994	0.051893
3		Apparent Polarity	0.042742	0.053714
4		Amplitude Weighted Cosine Phase	0.041411	0.050294
5		Second Derivative	0.040040	0.049241

The relatively small difference between training and validation errors confirms that the PNN model effectively generalizes the learned patterns to the entire seismic data set. This indicates that the selected combination of attributes adequately represents the key physical properties that control porosity variation in the Hugin Formation.

A summarized representation of these sequential procedures is shown in the workflow diagram in Figure 11.

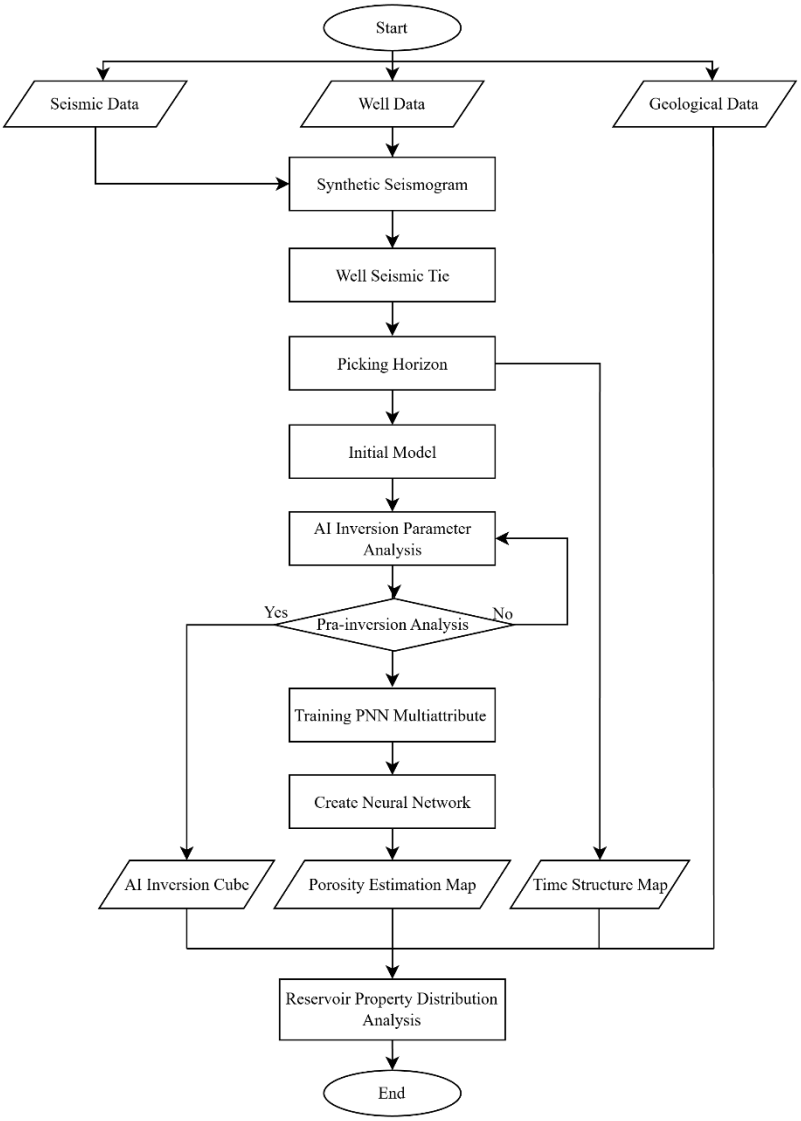

Figure 11 Research flow diagram

https://doi.org/10.35877/jetech4411

OPEN ACCESS

ISSN : 2776-7914 (Print) / 2807-3045 (Online)

4. Results and Discussion

The data used in the analysis include seismic volume, interpreted horizons, AI volume, and estimated porosity volume. This stage produced three main types of maps: Time Structure Map (TSM), AI maps, and porosity maps. To establish the structural framework controlling reservoir distribution in the study area, the mapped seismic horizons of the Hugin Formation were first analyzed in TWT to define the geometry of the top and base reservoir surfaces. TSM of the Top and Base Hugin horizons ranging from approximately 2,485 to 2,901 (ms). The structural configuration of both horizons shows a clear high to low pattern, where green indicates shallower high structures and purple represents deeper low structures. The contour geometry depicts a horst graben system, characterized by a Northwest-Southeast (NW-SE) trending depression bounded by higher blocks in the central part of the study area. The persistence of this central peak on both the Top and Base Hugin horizons indicates a cohesive vertical structural peak, which acts as a stable trapping configuration. These structural peaks are considered potential hydrocarbon traps, as their geometry is suitable for fluid accumulation within the Hugin reservoir interval. Overall, the configuration of the top and base Hugin horizons reinforces the presence of a structural in Figure 12.

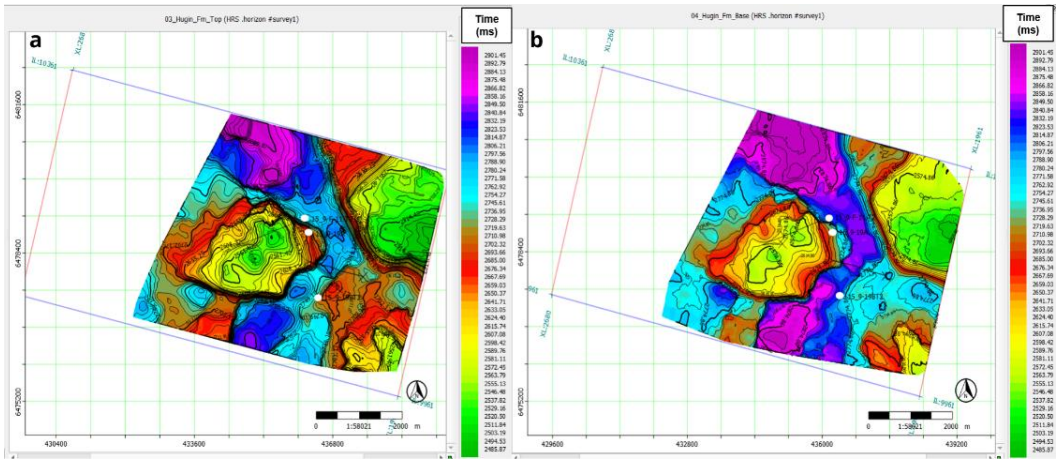

Figure 12 Time structure map (a) top (b) base

The integration of seismic inversion and multiattribute analysis provides a comprehensive quantitative approach for characterizing the Hugin Formation in the Volve Field, North Sea Basin. The Hugin Formation, deposited in a nearshore to shallow marine deltaic setting during the Middle Jurassic, consists predominantly of interbedded sandstone and shale sequences. Figure 13 displays the AI inversion section along the arbitrary seismic line that intersects the wells.

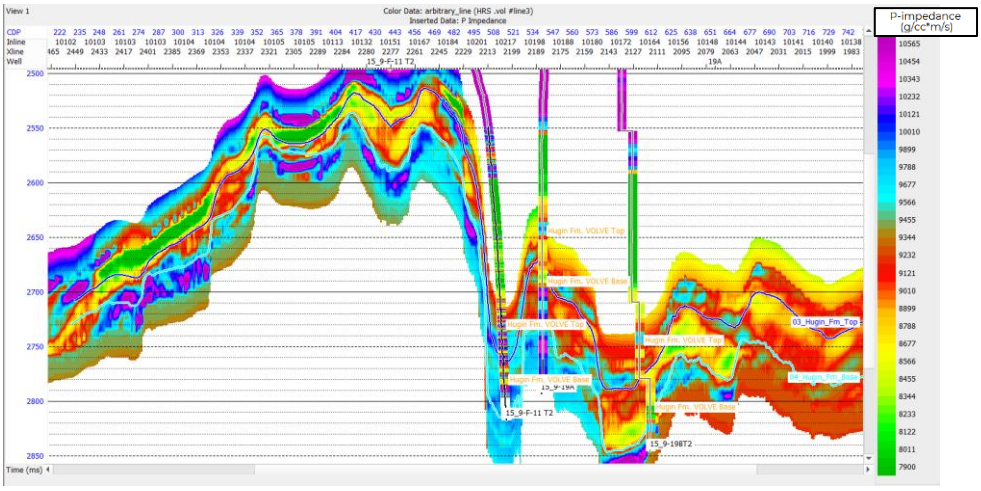

Figure 13 Model based AI inversion section along an arbitrary line

https://doi.org/10.35877/jetech4411

ISSN : 2776-7914 (Print) / 2807-3045 (Online)

From a quantitative interpretation perspective, the resulting impedance model effectively distinguishes between low impedance sandstone reservoirs values ranging from 7,000 to 9,000 (g/cc·m/s) and high impedance shale layers (>9,000 g/cc·m/s). The strong correspondence between the inverted AI logs and measured well data confirms the inversion's robustness and accuracy. The optimized parameters were subsequently adopted as the reference for the main inversion process, forming the quantitative foundation for further multiattribute and PNN based porosity prediction across the Hugin Formation. Figure 14 presents the validation plot comparing predicted porosity values obtained from the PNN model with the actual porosity measurements derived from well logs.

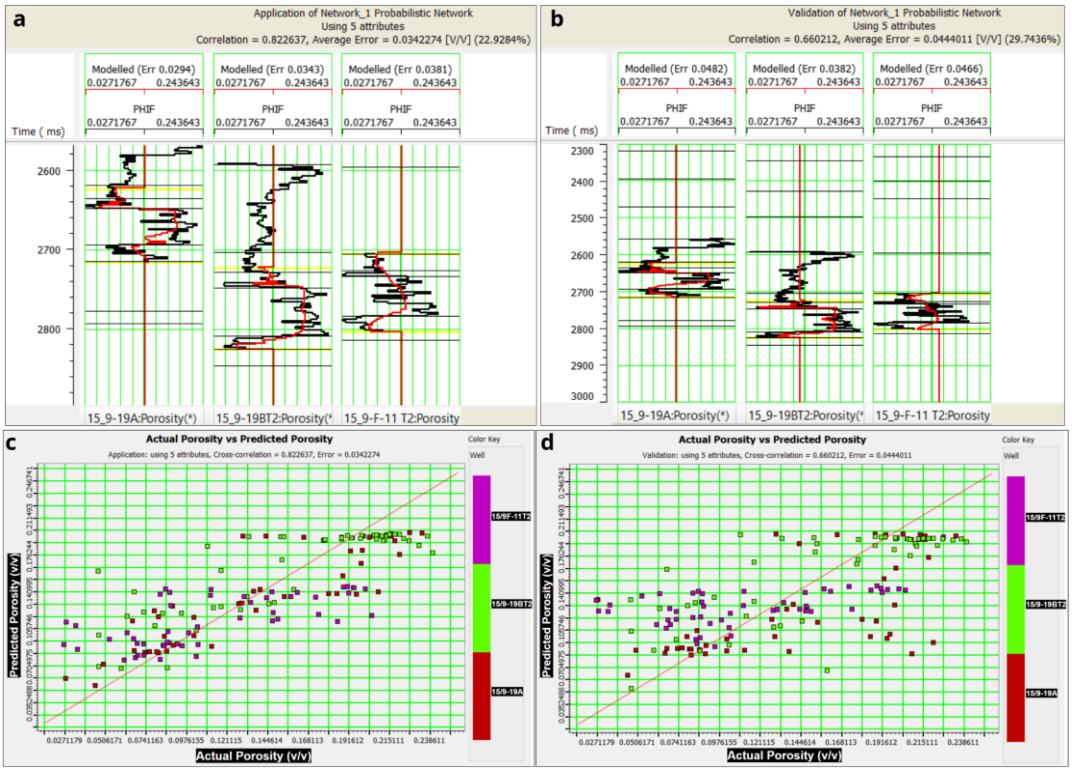

Figure 14 (a) Application of the PNN (b) validation of the PNN (c) crossplot correlation of PNN with cc = 0.82 (d) validation crossplot correlation of PNN with cc = 0.66

The crossplot shows a strong correspondence between predicted and measured porosity, as indicated by the regression trend line that closely matches the actual porosity trend from the well log. Correlation coefficients of approximately 0.82 for training and 0.66 for validation indicate that the PNN effectively captures the nonlinear relationship between seismic attributes and porosity. The limited spread of data points around the regression trend line indicates that prediction errors are small and randomly distributed, suggesting that the model is well generalized without showing signs of underfitting or overfitting. This validation result demonstrates that the combination of seismic attributes used likely including AI, RMS amplitude, reflection strength, and instantaneous frequency effectively represents the petrophysical variability within the Hugin Formation. The PNN, through its probabilistic classification framework, accurately maps these attribute variations into porosity predictions, even in zones where seismic amplitude responses are weak or ambiguous. Figure 15 presents the porosity estimation section derived from the seismic multiattribute analysis using the PNN method. The section illustrates the distribution of porosity across the seismic volume, with predicted values ranging from 0.1539 to 0.1956 (v/v). To obtain a clearer representation of porosity variations at each horizon, porosity slice were generated, producing porosity maps that allow the spatial patterns and reservoir quality trends to be interpreted more effectively.

https://doi.org/10.35877/jetech4411

ISSN : 2776-7914 (Print) / 2807-3045 (Online)

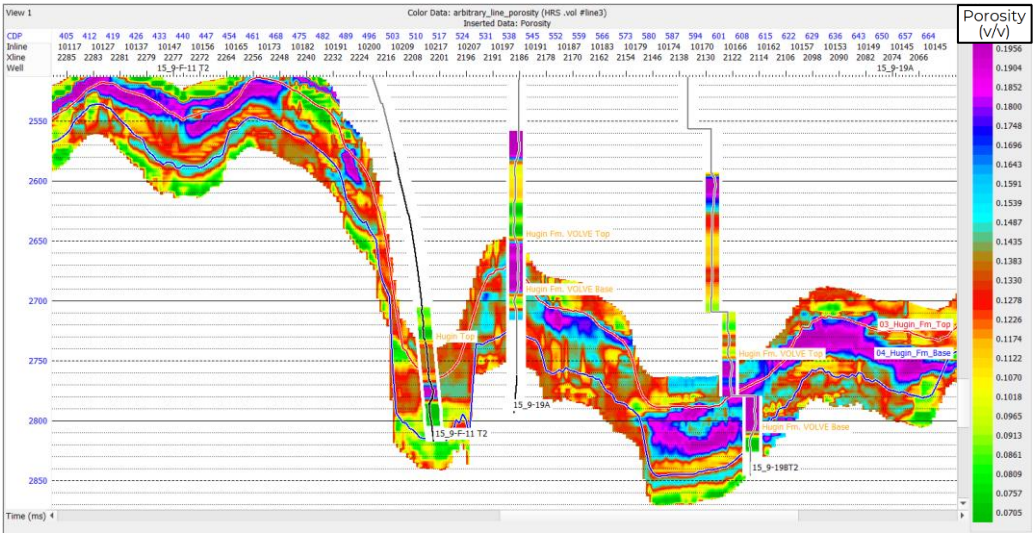

Figure 15 Porosity estimation section along an arbitrary line

Figure 16 compares the AI inversion slice map and the PNN derived porosity map within the top base Hugin Formation. The AI slice map reveals distinct impedance contrasts, where low impedance zones ranging from 7,000 to 9,000 (g/cc·m/s) are spatially correlated with high porosity intervals ranging from 0.1539 to 0.1956 (v/v). These zones indicate well developed sandstone reservoirs with good pore connectivity. Conversely, high impedance regions exceeding (9,000 g/cc·m/s) correspond to low porosity zones dominated by shale or cemented sandstone, which function as non-reservoir or cap rock units.

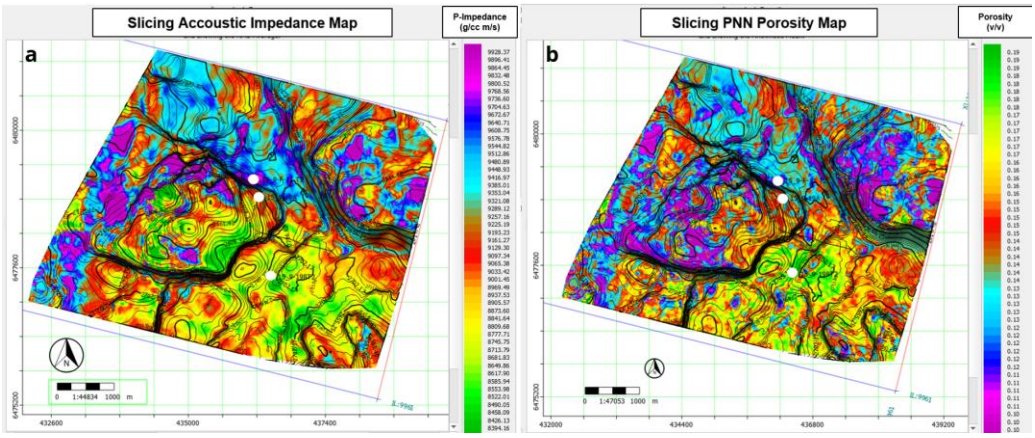

Figure 16 (a) AI slicing map (b) PNN porosity map

The spatial distribution patterns of impedance and porosity both reveal structural control, with NW-SE trending faults and gentle anticlinal closures forming potential hydrocarbon traps. The correspondence between these two datasets confirms the reliability of the inversion and PNN prediction results, showing that AI is an effective proxy for porosity in this lithologically heterogeneous setting.

The PNN porosity map demonstrates a strong alignment with the predicted geological facies distribution. High porosity regions are concentrated in the central and northeastern parts of the study area, consistent with the proximal to medial deltaic deposits within the conceptual model. The porosity decreases toward the southwestern and eastern flanks, indicating the influence of diagenetic compaction and reduced grain sorting. This trend is coherent with the sediment dispersal direction inferred from the conceptual model, which suggests southwest-northeast progradation of deltaic lobes. The high correlation coefficient (training cc = 0.82; validation cc = 0.66) further supports that the PNN successfully captures the nonlinear relationship between seismic attributes and petrophysical parameters, thus producing reliable

https://doi.org/10.35877/jetech4411

ISSN : 2776-7914 (Print) / 2807-3045 (Online)

porosity predictions. Figure 17 integrates the AI and porosity maps with the conceptual geological model of the Hugin Formation.

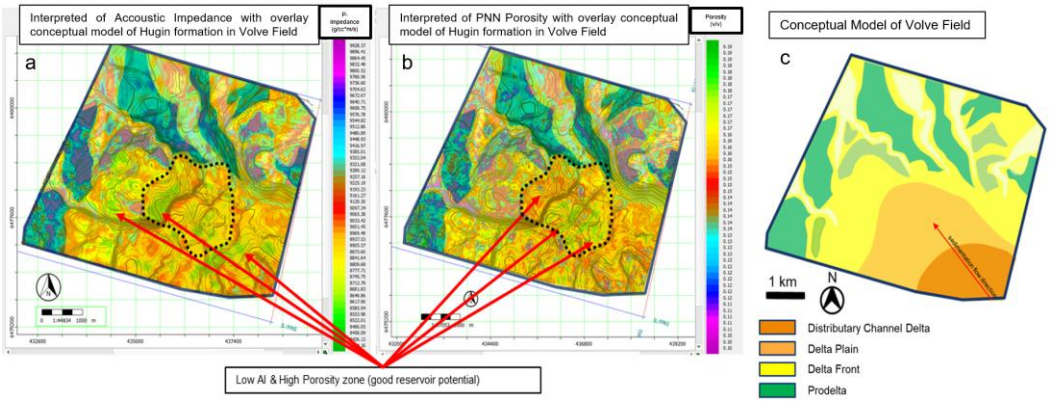

Figure 17 (a) AI slicing map (b) PNN porosity map (c) depositional conceptual model map

This composite visualization depicts the spatial continuity of the reservoir zone and its relationship to the structural and stratigraphic framework. This conceptual model depicts a shallow coastal marine delta system where distribution channels and mouth bars dominate the reservoir facies. This sandstone body is intersp ersed with transgressive shale layers, which act as vertical seals. The anticline structure in the central zone, which is parallel to the regional fault system, acts as the main structural trap. The integration of seismic derived impedance and porosity maps in this conceptual model refines the understanding of facies distribution and reservoir geometry. The observed low impedance and high porosity anomalies correspond to the predicted delta front sandstone bodies, while higher impedance areas represent interdistributary or marine shale facies.

This integrated interpretation highlights the strong interaction between structural configuration, depositional facies, and petrophysical heterogeneity. AI inversion effectively depicts lithological boundaries, while PNN based porosity prediction improves the resolution of reservoir property estimation. Simultaneously, these methods validate the conceptual model by showing that the Hugin Formation reservoir is laterally continuous but vertically heterogeneous due to differences in compaction and diagenesis. This integration also shows that reservoir quality improves towards the structural peak and central delta lobe, where sandstone thickness and sorting are optimal. This improves understanding of reservoir distribution, refines the delineation of hydrocarbon bearing zones, and reduces uncertainty in structural and facies interpretation.

5. Conclusion

Model based AI seismic inversion integrated with PNN multiattribute analysis has effectively characterized the Hugin Formation in the Volve Field. The main conclusions are as follows:

1. The Hugin Formation sandstone reservoirs exhibit low AI values ranging from 7,000 to 9,000 (g/cc·m/s) and high porosity values ranging from 0.15 to 0.30 (v/v), representing well sorted and highly porous sandstone facies. In contrast, high impedance zones (>9,000 g/cc·m/s) correspond to shale and compacted lithologies that act as non-reservoir or cap rock layers.
2. The geometry and quality of the reservoir are significantly influenced by NW-SE trending faults and anticline structures due to the presence of salt domes beneath the formation and older formations, which create effective structural traps and compartmentalized reservoir zones. These structural elevations correlate with low impedance anomalies and high porosity, confirming the relationship between structural control and stratigraphy.
3. The integration of impedance maps generated from inversion and porosity maps predicted by PNN provides a consistent geological framework that validates the Hugin Formation deltaic deposition model. This workflow not only improves reservoir mapping and

https://doi.org/10.35877/jetech4411

ISSN : 2776-7914 (Print) / 2807-3045 (Online)

hydrocarbon prospect identification, but also offers an applicable, data driven methodology for reservoir characterization in other deltaic and shallow marine environments in the North Sea Basin.

Acknowledgements

The authors express their sincere appreciation to the Volve Field Norway consortium, Equinor ASA, ExxonMobil E&P Norway AS, and Bayerngas Norge AS, for providing open access to the complete Volve Field dataset through the Equinor Data Sharing Portal. The availability of high quality 3D seismic data, well logs, production information, reservoir models, and supporting technical documents formed an important foundation for this research and significantly strengthened the analytical robustness and scientific reliability of this study. The authors are grateful for the consortium's commitment to transparency and data sharing, which continues to support global progress in the fields of geoscience and reservoir engineering.

References

Ardinda, F., & Riyanto, A. (2020). Seismic multi-attribute analysis for petrophysics reservoir prediction with probabilistic neural network in "fA" field. E3S Web of Conferences, 200. https://doi.org/10.1051/e3sconf/202020006010

Chasandra, B., Dewanto, O., & Juniari, P. (2018). Karakterisasi Reservoar Melalui Analisis Petrofisika Berdasarkan Data Log Sumur " TRD " FORMASI AIR BENAKAT PT Pertamina EP ASSET 1 Jambi Sub-Cekungan Dibatasi Oleh Sub-Cekungan Palembang Sumatera Selatan Sangat Dikontrol Oleh Dipengaruhi Oleh Pergerakan. Jurnal Geofisika Eksplorasi, 4(1), 60–72. https://doi.org/10.23960/jge.v4i1.

Leite, E. P., & Vidal, A. C. (2011). 3D porosity prediction from seismic inversion and neural networks. Computers & Geosciences, 37(8), 1174–1180. https://doi.org/https://doi.org/10.1016/j.cageo.2010.08.001

Pelemo-Daniels, D., & Stewart, R. R. (2024). Petrophysical Property Prediction from Seismic Inversion Attributes Using Rock Physics and Machine Learning: Volve Field, North Sea. Applied Sciences (Switzerland), 14(4). https://doi.org/10.3390/app14041345

Person, C., & Peter, N. (1998). Geology of the North Sea. In North.

Rizqi, M. I. F., & Firdaus, R. (2021). Karakterisasi reservoir menggunakan metode Seismik Inversi Acoustic Impedance (AI) dan Seismik Multiatribut dengan Probabilistic Neural Network (PNN) pada lapangan Blok F3, North Sea Netherland. Journal of Science and Applicative Technology, 5(2), 274. https://doi.org/10.35472/jsat.v5i2.274

Sanderson, D. J. (1991). Interpretation of Three-dimensional Seismic Data. Journal of Structural Geology, 13(1), 121–122. https://doi.org/10.1016/0191-8141(91)90111-u

Specht, D. F. (1990). Probabilistic neural networks. Neural Networks, 3(1), 109–118. https://doi.org/https://doi.org/10.1016/0893-6080(90)90049-Q

Zwaan, F., Schreurs, G., Buiter, S. J. H., Ferrer, O., Reitano, R., Rudolf, M., & Willingshofer, E. (2022). Analogue modelling of basin inversion: a review and future perspectives. Solid Earth, 13(12), 1859–1905. https://doi.org/10.5194/se-13-1859-2022